Biosensors and Bioelectronics 216 (2022) 114624

Contents lists available at ScienceDirect

Biosensors and Bioelectronics

journal homepage: www.elsevier.com/locate/bios

EdU sensing: The Raman way of following endothelial cell proliferation *in vitro* and *ex vivo*

Basseem Radwan [a,b], Stefano Rocchetti [a], Ewelina Matuszyk [a], Magdalena Sternak [a], Maciej Stodulski [c], Robert Pawlowski [c], Jacek Mlynarski [c], Krzysztof Brzozowski [b], Stefan Chlopicki [a,d], Malgorzata Baranska [a,b,*]

[a] Jagiellonian Centre for Experimental Therapeutics (JCET), Jagiellonian University, 14 Bobrzynskiego Str, 30-348, Krakow, Poland
[b] Faculty of Chemistry, Jagiellonian University, 2 Gronostajowa Str, 30-387, Krakow, Poland
[c] Institute of Organic Chemistry, Polish Academy of Sciences, 44/52 Kasprzaka Str, 01-224, Warsaw, Poland
[d] Jagiellonian University, 30-348, Krakow, Poland

ARTICLE INFO

Keywords:
Raman imaging
Click chemistry
Fluorescence imaging
Endothelium
Cell proliferation
Cycloheximide
Doxorubicin

ABSTRACT

Endothelial cells line the lumen of all vessels in the body and maintain vascular homeostasis. In particular, endothelial cell regeneration in response to insult sustain functional endothelial layer. EdU (5-ethynyl-2′-deoxyuridine) is an alkyne-tagged proliferation probe that incorporates into newly synthesized DNA and is used for fluorescence imaging of cell proliferation with the use of "click chemistry" reaction with a fluorescent azide. Here, we utilized EdU as a click-free Raman probe for tracking endothelial cell proliferation. Raman imaging of EdU was performed in live endothelial cells, showing an advantage over fluorescence imaging of EdU, as this technique did not require sample fixation and permeabilization. To validate Raman-based imaging of EdU to study endothelial cell proliferation, we showed that when endothelial cells were treated with cycloheximide or doxorubicin to impair the proliferation of endothelial cells, the Raman-based signal of EdU was diminished. Furthermore, endothelial cells proliferation detected using EdU-labelled Raman imaging was compared with fluorescence imaging. Finally, the method of Raman–based EdU imaging was used in the isolated murine aorta *ex vivo*. Altogether, our results show that Raman-based imaging of EdU provides a novel alternative for fluorescence-based assay to assess endothelial proliferation and regeneration.

1. Introduction

Endothelial cells (EC) form a monolayer lining the lumen of all vessels in the body. They play a significant role in maintaining cardiovascular homeostasis through their multiple endocrine, paracrine, and autocrine functions (Daiber and Chlopicki, 2020; Galley and Webster, 2004; Walczak et al., 2015). EC are involved in the regulation of blood flow, vascular permeability, smooth muscle cells proliferation, inflammatory response, thrombosis and angiogenesis (Rajendran et al., 2013) and the impairment in the endothelial regulatory function results in endothelial dysfunction (ED) (Cau et al., 2018). ED has been linked to the development of many diseases such as atherosclerosis, diabetes, hypertension, liver disease cancer or COVID-19 (Huertas et al., 2020; Maslak et al., 2015; Rajendran et al., 2013; Ruhl et al., 2021; Smeda et al., 2020; Smeda and Chlopicki, 2020) and the phenotype of ED is often associated with an altered capacity of endothelial regeneration unable to repair vascular dysfunction (Deanfield et al., 2007). Therefore, tracking the proliferation of EC, particularly in *in vivo* and *ex vivo* conditions, provides an important insight into the endothelial phenotype and is usually done with the use of EdU assay.

5-ethynyl-2′-deoxyuridine (EdU) is an alkyne-tagged thymidine analogue that incorporates into newly synthesized DNA during replication (Salic and Mitchison, 2008). As a result of the copper-catalysed azide-alkyne cycloaddition reaction, i.e. "Click chemistry" with a fluorescent azide, EdU has been used in fluorescence imaging to follow DNA synthesis of proliferating cells (Basile et al., 2011; Ishizuka et al., 2016). This technique demonstrates the great advantage of not relying on an antibody to label DNA, omitting the need for the rigorous step of DNA denaturation (Salic and Mitchison, 2008). However, due to the cytotoxicity of the copper catalyst and the poor permeability of the

* Corresponding author. Jagiellonian Centre for Experimental Therapeutics (JCET), Jagiellonian University, 14 Bobrzynskiego Str, 30-348, Krakow, Poland.
E-mail address: m.baranska@uj.edu.pl (M. Baranska).

https://doi.org/10.1016/j.bios.2022.114624
Received 10 June 2022; Received in revised form 25 July 2022; Accepted 3 August 2022
Available online 10 August 2022

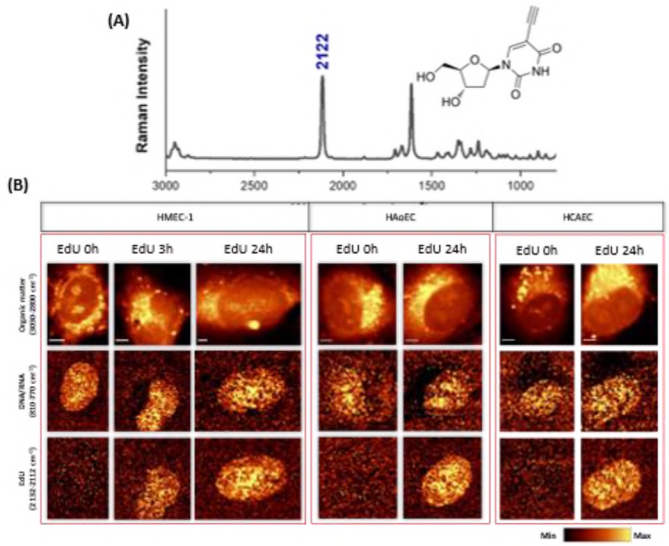

Fig. 1. EdU as an alkyne-tagged Raman probe for detection of DNA in EC of various origins e.g. in human microvascular endothelial cells (HMEC-1), human aortic endothelial cells (HAoEC) and human coronary artery endothelial cells (HCAEC). **(A)** Structure and Raman spectrum of 5-Ethynyl-2′-deoxyuridine (EdU). **(B)** Raman image of control and EdU-tagged HMEC-1 (0, 3 and 24h), HAoEC, and HCAEC cells (0 and 24h), obtained by the integration of Raman bands over the selected spectral regions: 3030–2800 cm^{-1} (organic matter), 810–770 cm^{-1} (DNA/RNA), and 2132–2112 cm^{-1} (Alkyne group, EdU). Scale bars equal 5 μm.

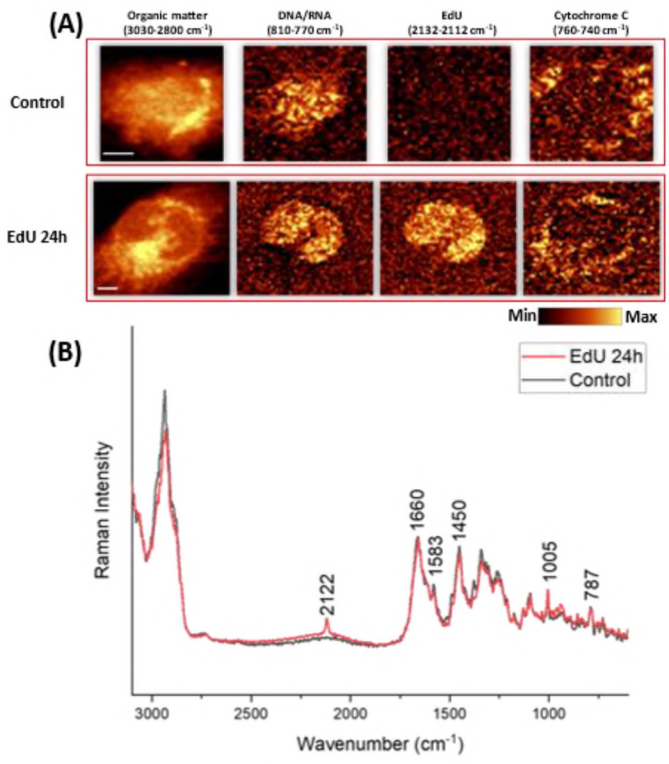

Fig. 2. Live cell Raman imaging of EdU-tagged HMEC-1. (A) Raman images of control and EdU-labelled HMEC-1 were obtained by the integration of Raman bands at 3030–2800 cm^{-1} (organic matter), 810–770 cm^{-1} (DNA/RNA), 2132–2112 cm^{-1} (Alkyne group, EdU), and 760–740 cm^{-1} (Cytochrome C). Scale bars equal 5 μm. **(B)** Averaged spectra of the nucleus class of the control (grey) and EdU-labelled (red).

fluorescent azide dyes, sample fixation and permeabilization are needed for proliferation detection.

As an alternative to the fluorescence-based analysis, Raman imaging can be considered. Raman spectroscopy is regarded as a powerful tool in the detection of key biological compounds i.e. proteins, lipids, and nucleic acids within cell and tissue models of various diseases in a label-free manner, omitting the undesirable influence that dyes may have on samples (Adamczyk et al., 2021). On the other hand, the use of Raman probes (Rp) has been shown to improve selectivity in subcellular organelles imaging and tracking specific molecules, and to some extent, the sensitivity of this approach is greater than the measurements without probes (Adamczyk et al., 2021; Czamara et al., 2021; Matuszyk et al., 2021; Radwan et al., 2020). Rp are usually small molecules that ideally have a targeting moiety that marks specific subcellular structures or molecules and a Raman reporting moiety that improves Raman detection by signal enhancement or demonstrating a band in the silent spectral region (ca. 2800–1800 cm^{-1}). In this regard, EdU represents an Rp as this molecule can be easily detected in cells due to the alkyne tag being a part of its structure that gives a Raman band at ca. 2122 cm^{-1} in the "silent region", where there is no interference with the signal from other cellular components (Yamakoshi et al., 2011). Furthermore, Raman-based detection of EdU-tagged DNA could be done in a click-free manner, i.e. DNA could be identified in the Raman spectra based on incorporated EdU into biological samples without the need for any additional dyes, therefore, allowing live-cell imaging. This is not possible using the fluorescence-based detection approaches that rely on the click chemistry reaction between EdU and a fluor azide dye following cell fixation and permeabilization.

EdU incorporation into the double-stranded DNA and its content in the nucleus increases with cell proliferation, providing enhanced Raman signal derived from EdU when imaging cell nuclei. This has been already demonstrated when imaging HeLa cells incubated with EdU for 21 h (Yamakoshi et al., 2011). As a thymidine analogue, EdU incorporates specifically into cellular DNA, therefore, the detection of EdU allows monitoring cellular DNA solely, while it is difficult to isolate signals from cellular DNA and RNA using label-free Raman techniques.

Indeed, Raman imaging of EC provides valuable information on the phenotype and chemical changes in endothelial cells (Adamczyk et al., 2021; Baranska et al., 2015) including the chemical composition of cellular nucleic acids by identifying the Raman bands at ca. 788 cm^{-1} (phosphodiester bonds in DNA), 813 cm^{-1} (phosphodiester bonds in RNA), and 1095 cm^{-1} (phosphodioxy group, PO_2^-) using label-free Raman techniques (Adamczyk et al., 2021). However, investigating cell proliferation and the state of newly synthesized DNA could not be achieved with the label-free Raman methods. Here we present an approach to analysing newly synthesized DNA based on EdU-tagged DNA in EC and its band arising at ca. 2122 cm^{-1}, permitting the investigation of cell proliferation, while at the same time keeping the information obtained from the bands associated with nucleic acids intact. This method was used to detect endothelial cell proliferation in healthy endothelial cells and in endothelial cells when proliferation was impaired by cycloheximide (CHX) or doxorubicin (DOX). CHX, an antifungal antibiotic, is a protein synthesis inhibitor that is widely used in *in vitro* studies (SIEGEL and SISLER, 1963). When cells are treated with CHX for short incubation times, it leads to the inhibition of the cellular DNA synthesis by stalling replication forks due to protein deprivation (Henriksson et al., 2018; Liu et al., 2010). Doxorubicin (DOX), an anthracycline antibiotic used in cancer treatment, endowed with cardiotoxicity (Liu and Melchert, 2010) is thought to directly damage DNA through intercalation and inhibition of topoisomerase II (Taymaz-Nikerel et al., 2018). DOX treatment leads to DNA fragmentation, inhibition of cell proliferation and apoptosis (Kim et al., 2009). Previous spectroscopic studies of the effects of CHX and DOX treatments on EC have demonstrated the chemical and morphological changes associated with these compounds (Czamara et al., 2016; Majzner et al., 2015; Wojcik et al., 2015). However, their effect on EC proliferation

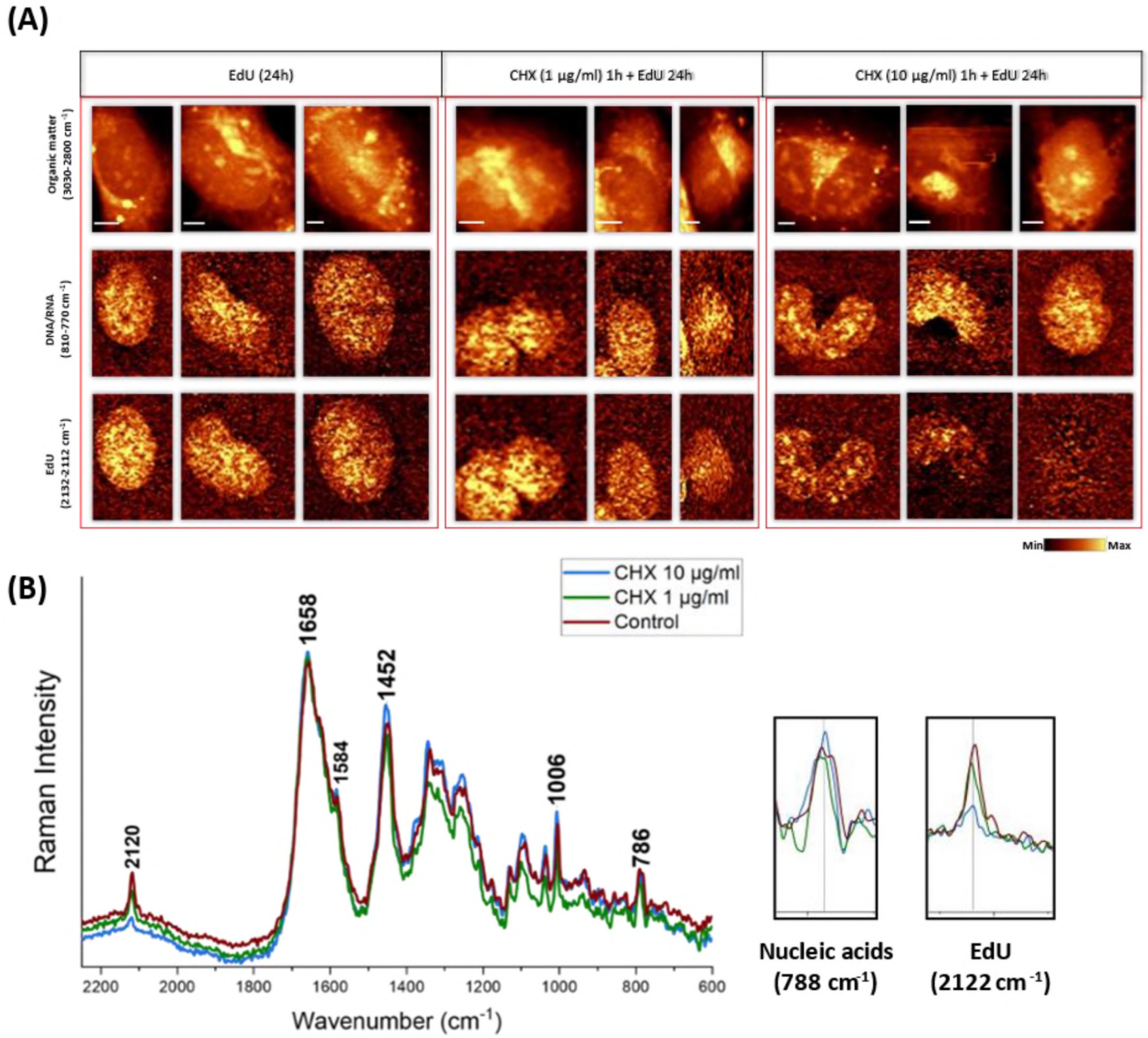

Fig. 3. Raman images of EdU-tagged HMEC-1 with and without CHX pre-treatment. **(A)** Raman images of EdU-labelled (20 µM, 24h) control and CHX pre-treated (1 and 10 µg/ml, 1h) HMEC-1 constructed by the integration of Raman bands at: 3030–2800 cm^{-1} (organic matter), 810–770 cm^{-1} (DNA/RNA), 2132–2112 cm^{-1} (Alkyne group, EdU). **(B)** average spectra of EdU-labelled nuclei class obtained by KMCA of control (red) and cells pre-incubated CHX in 1 µg/ml (green) and 10 µg/ml (blue) showcasing the bands at ca. 788 cm^{-1} (nucleic acids) and 2122 cm^{-1} (EdU).

studied with Raman imaging has not been studied before.

Here, we present the Raman–based approach to assay cell proliferation utilizing EdU as a click-free Raman probe for DNA replication. Fluorescence detection of Alexa Fluor®-stained EdU is used as a reference method. As a proof of concept, we studied endothelial proliferation in endothelial cell culture while endothelial cell regeneration was studied in isolated murine aortae.

2. Materials and methods

2.1. Cell culture

HMEC-1 between passages 2 and 6 were used in all the Raman and fluorescence experiments to detect cell proliferation, with and without CHX pre-treatment. Cells were cultured in a complete MCDB131 medium (Gibco Life Technologies) supplemented with 10 mM L-glutamine (Gibco Life Technologies), 1 µg/mL hydrocortisone (Sigma Aldrich), 10 mg/mL epidermal growth factor (EGF, Sigma Aldrich), 10% fetal bovine serum (FBS, Gibco Life Technologies) and antibiotic antimycotic solution (AAS with 10.000 U penicillin, 10 mg streptomycin, and 25 µg amphotericin B per mL). Additionally, two more EC lines were used for EdU labelled Raman imaging of their DNA, i.e. primary human aortic endothelial cells (HAoEC) and human coronary artery endothelial cells (HCAEC). They were cultured in a complete EGM-2MV medium (Lonza, Basel, Switzerland), supplemented with 10 mM L-glutamine (Gibco Life Technologies), 1 µg/mL hydrocortisone (Sigma Aldrich, St. Louis, MO, USA), 10 mg/mL epidermal growth factor (EGF, Sigma Aldrich), 10% fetal bovine serum (FBS, Gibco Life Technologies) and 1% of antibiotics (streptomycin, penicillin and fungison, Gibco Life Technologies). The cell cultures were incubated in a 37 °C, 5% CO_2/95% air

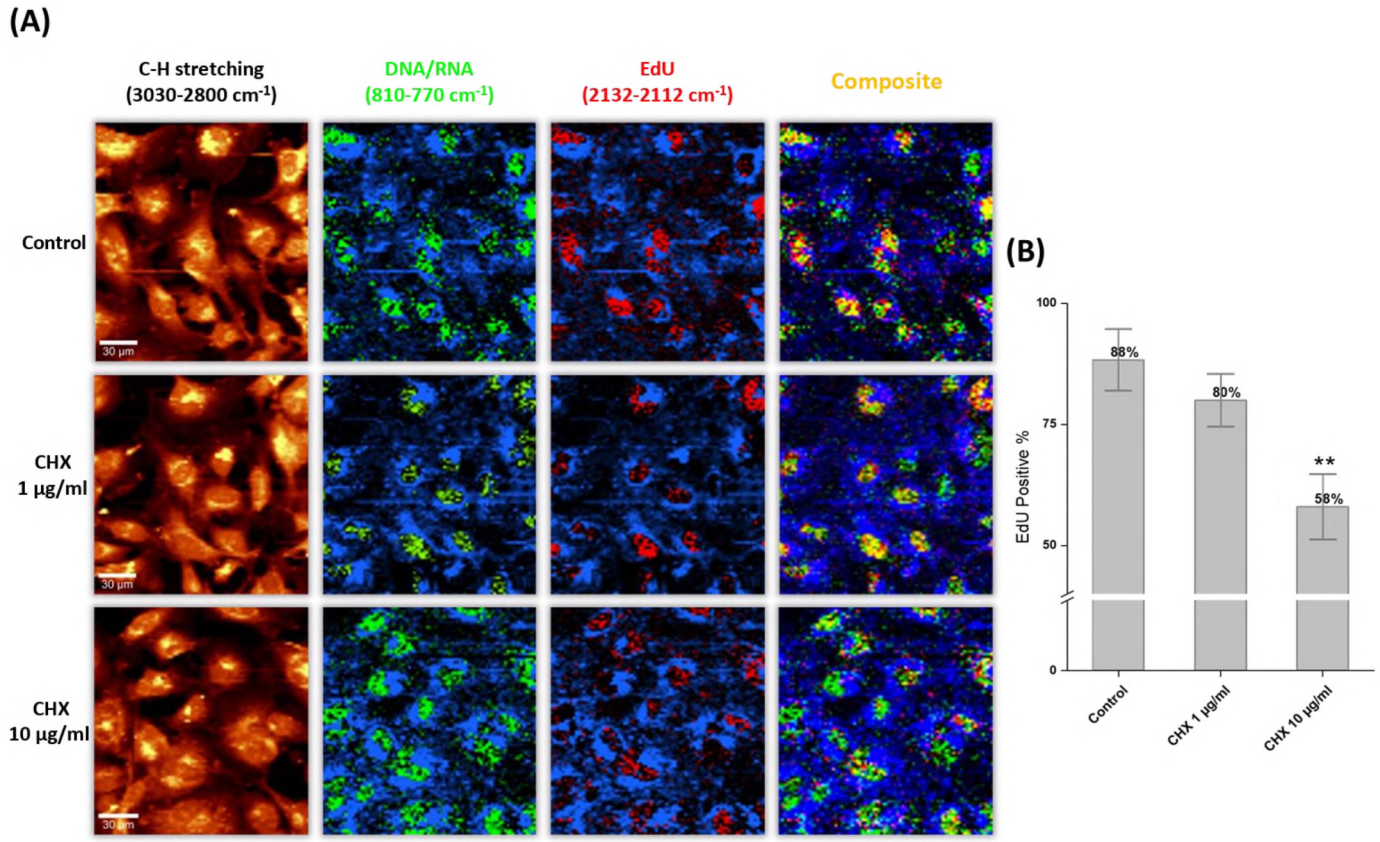

Fig. 4. Raman imaging-based quantification of EC proliferation inhibition following CHX treatment (A) Raman images of EdU tagged HMEC-1 were obtained by the integration of Raman bands over the spectral regions: 3030–2800 cm^{-1} (organic matter, blue), 810–770 cm^{-1} (DNA/RNA, green), 2132–2112 cm^{-1} (Alkyne group; EdU, red) and composite images (overlapping between EdU and nucleic acids signal in yellow). Showing EdU distribution in EC nuclei with and without CHX pre-treatment. Scale bars equal 30 µm. **(B)** percentage of EdU-positive HMEC-1 cells (that express a Raman band at ca. 2122 cm^{-1}) to the total number of cells (based on the nucleic acids band at ca. 788 cm^{-1}) presented as means ± SD from 3 independent experiments, n = 50 ± 2 cells/group. **P < 0.01 vs. control.

humidified cell culture incubator.

For the Raman experiments, HMEC-1, HAoEC, and HCAEC were seeded directly onto Calcium Floride (CaF_2) windows to reach optimal confluency after 24 h. For studying cell proliferation HMEC-1 cells were either pre-treated with CHX (1 and 10 µg/mL) for 1 h or incubated in a CHX-free medium, afterwards, cells were incubated with EdU (20 µM) in a cell culture medium for 3 or 24h. HAoEC and HCAEC were either incubated with EdU (20 µM) for 24h or with the EdU-free medium. Live cell imaging was performed, or cells were fixed (2.5% glutaraldehyde) and stored at 4 °C until measurements.

For fluorescence imaging, cells in culture were plated in 96-well plates to be confluent after 24 h. On the day of the experiment, cells were treated with CHX (at concentrations 1 and 10 µg/mL) for 1 h and then incubated with EdU dilution in the cell culture medium (10 µM) for either 1 or 24 h.

2.2. Aorta tissue

All experiments involving animals described in the present study were approved by the Local Jagiellonian University Ethical Committee on Animal Experiments in accordance with the Guidelines for Animal Care and Treatment of the European Community.

Male C57Bl/6 (wild type) aged 8–12 weeks were intraperitoneally injected with EdU (150 mg/kg body weight) every other day for a week. Afterwards, the animals were anaesthetized by an intraperitoneal injection of a mixture consisting of ketamine and xylazine (100 mg ketamine/10 mg xylazine/kg body weight). The thoracic aortae were isolated and transferred into Krebs–Henseleit buffer, then cleaned from the surrounding tissue and cut into rings of ca. 1–2 mm. A group of the aortic rings was subjected to mechanical injury with a sharp object. Next, aortic rings were incubated for 48 h (at 37°C and 5% CO_2) in minimal essential medium (MEM) with EdU (200 µM) supplemented with 1% MEM vitamins, 1% antibiotics (penicillin 10,000 U/mL and streptomycin 10,000 µg/mL), 1% non-essential amino acids, and 20% fetal bovine serum (FBS). The aortic rings were incubated in media with and without vascular endothelial growth factor (VEGF; Sigma Aldrich) supplementation. Later, the rings were split open and mounted on Cell-Tak®-coated glass slides or calcium fluoride slides for subsequent Fluorescence and Raman measurements respectively. Samples were washed in PBS and fixed using 4% paraformaldehyde (for fluorescence imaging) or 4% formalin solution (for Raman imaging) for 15 and 10 min respectively. *En face* aorta samples prepared for Raman imaging were stored in PBS at 4°C until being measured without any further staining.

Before immunostaining, the aortae samples were blocked with TNB blocking buffer (0.1 M Tris-HCl pH 7.5, 0.15 M NaCl, and 0.5% (w/v) blocking reagent (PerkinElmer FP1020)) for 4h. Afterwards, samples were permeabilized using 0.5% Triton-X 100 in PBS, washed with PBS, and incubated in a click reaction cocktail (prepared according to the manufacturer instructions) containing Alexa Fluor® 555 azide for subsequent EdU detection. Aortae samples were washed thoroughly and incubated with anti-CD31 antibody (Abcam, 1:50) diluted in TNB blocking buffer overnight at 4 °C. Then, they were washed in PBS and incubated with Alexa Fluor 647 goat-anti-rabbit (Immunoresearch Laboratories, 1:200) at room temperature in the dark for 3h. Finally, Hoechst 33258 (Sigma Aldrich; 1:1000) was used to stain samples' nuclei. Aortae samples were covered with glass coverslips, protected from light, and measured using CQ1 Confocal Quantitative Image

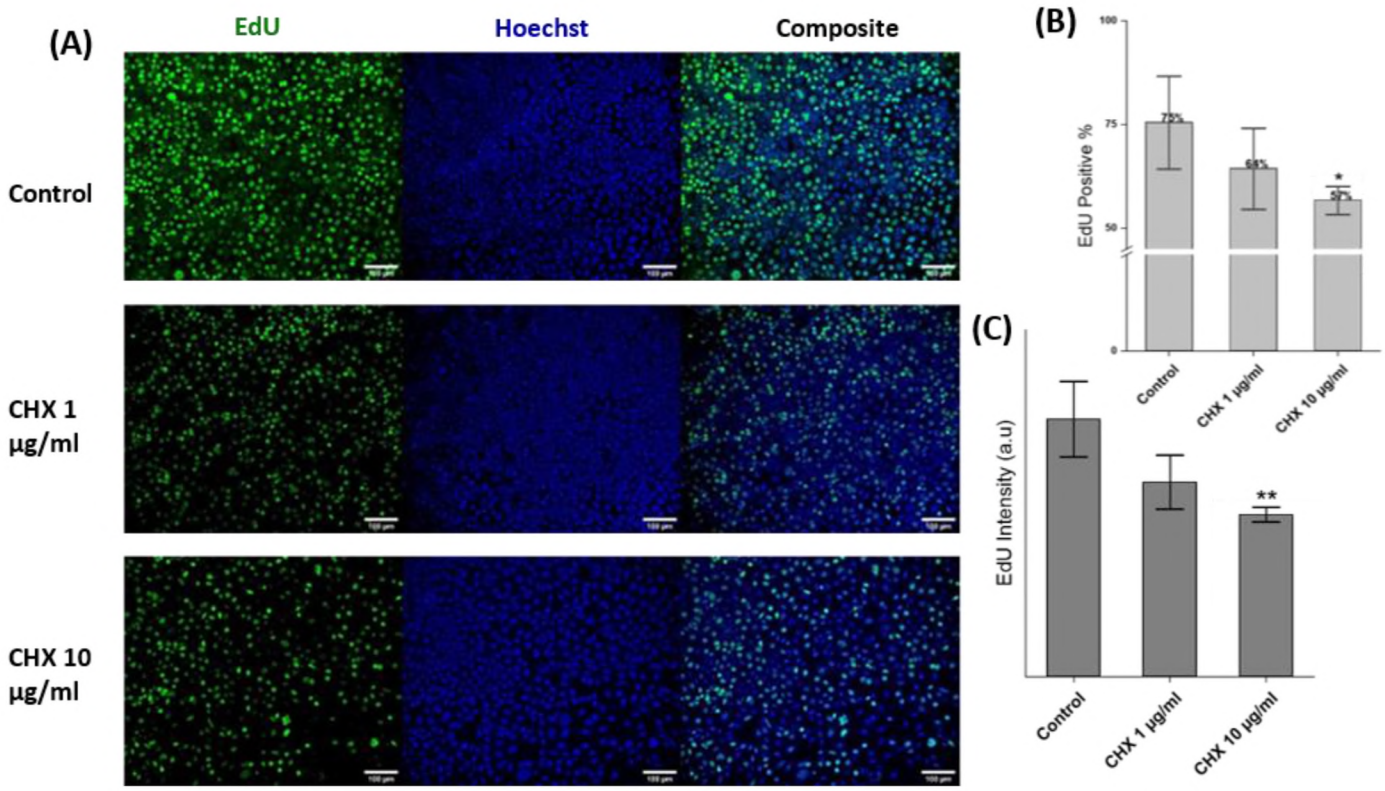

Fig. 5. Fluorescence imaging of Alexa fluor® 488-tagged EdU as a reference method. (A) Fluorescent images showing EdU positive cells nuclei (green), total nuclei in the samples (Hoechst, blue), and composite images of EdU-tagged control and CHX (1 and 10 μg/ml) pre-treated HMEC-1. Scale bars equal 100 μm **(B)** Total percentage of EdU-positive HMEC-1 calculated over the total number of Hoechst-stained nuclei, and **(C)** the average intensity of the overall fluorescent signal obtained from Alexa fluor® 488 signalling EdU in cell nuclei of the control and CHX pre-treated cells. The results are presented as the means ± SD from 3 independent experiments, *P < 0.05, **P < 0.01 vs. control.

Cytometer (Yokogawa; 20 × magnification objective).

2.3. Raman imaging

Raman imaging of all samples was performed using a WITec alpha 300 Confocal Raman Imaging system (WITec GmbH, Ulm, Germany) equipped with an Ultra-High-Throughput Screening (UHTS) 300 spectrograph, a charge-coupled device (CCD) detector (Andor, DU401A-BV-352), and an air-cooled solid-state laser with an excitation wavelength of 532 nm (or 488 nm for DOX experiments) was used to excite the samples. A 60 × water immersion objective (Nikon Fluor, NA = 1.0) was used for single-cell imaging, the spectra of cells were obtained using 0.5 s integration time and a 0.5 μm step size. Whereas for imaging a larger area, a 40 × water immersion objective (Zeiss, NA = 1.0) was used to obtain spectra at 0.3 s integration time and 2 μm step size. Imaging of the *en face* aortae samples was performed using the 60 × water immersion objective (Nikon Fluor, NA = 1.0), with an integration time of 0.3 s and a step size of 0.5 μm.

2.4. EdU click chemistry assay and fluorescence imaging

In order to fluorescently label the incorporated EdU in HMECs, cells were fixed using 4% paraformaldehyde solution for 10 min. After the washing step with 3% BSA in PBS, cells were permeabilized using 0.5% Triton-X 100 in PBS for 20 min, and they were washed again. Then, cells were incubated for 30 min in the dark with a reaction cocktail prepared according to the manufacturer's instruction, which contains the compounds necessary for the bonding of Alexa Fluor® 488 azide with EdU. After an additional washing step using PBS, cell nuclei were stained with Hoechst 33342 (1:1000 in PBS) for 10 min and then washed. For the imaging procedure, the Confocal Quantitative image cytometer (CQ1, Yokogawa) was used. Laser lines at 405 nm and 488 nm with emission filters FF01-452/45 and BP525/50 were used to collect images from cell nuclei and incorporated EdU, respectively.

2.5. Data analysis

Obtained Raman spectra were processed by a routine cosmic ray removal and were baseline corrected using auto-polynomial of degree 3 using WITec Project Plus software. To extract the average spectra of cell nuclei from different groups, Cluster analysis (CA) was performed with the k-means method (k-means cluster analysis, KMCA) using the Manhattan distance (WITec Project Plus software). Origin Pro 2022 was used for normalizing and presenting the spectra.

ImageJ (National Institutes of Health; http://rsbweb.nih.gov/ij/) and Columbus software were used for the processing of the fluorescence images. The total number of cells (based on Hoechst staining) the number of EdU-positive cells and the average fluorescence intensity were calculated. Whereas for the Raman imaging-based proliferation assay, the total number of cells and the number of EdU-positive cells were calculated based on the nucleic acids band at ca. 788 cm^{-1} and the alkyne band at ca. 2122 cm^{-1} respectively. To determine the statistical significance a two-sample *t*-test was used (Origin Pro, 2022).

3. Results and discussion

3.1. Locating DNA in the cell by detecting EdU

EdU-tagged Raman-based detection of EC nuclei in HMEC-1 cells was performed upon incubation with EdU for 0, 3, and 24 h. The most intense band of EdU arising from the alkyne tag was seen at ca. 2122 cm^{-1} (Fig. 1A) and was used to characterise cellular EdU distribution. A

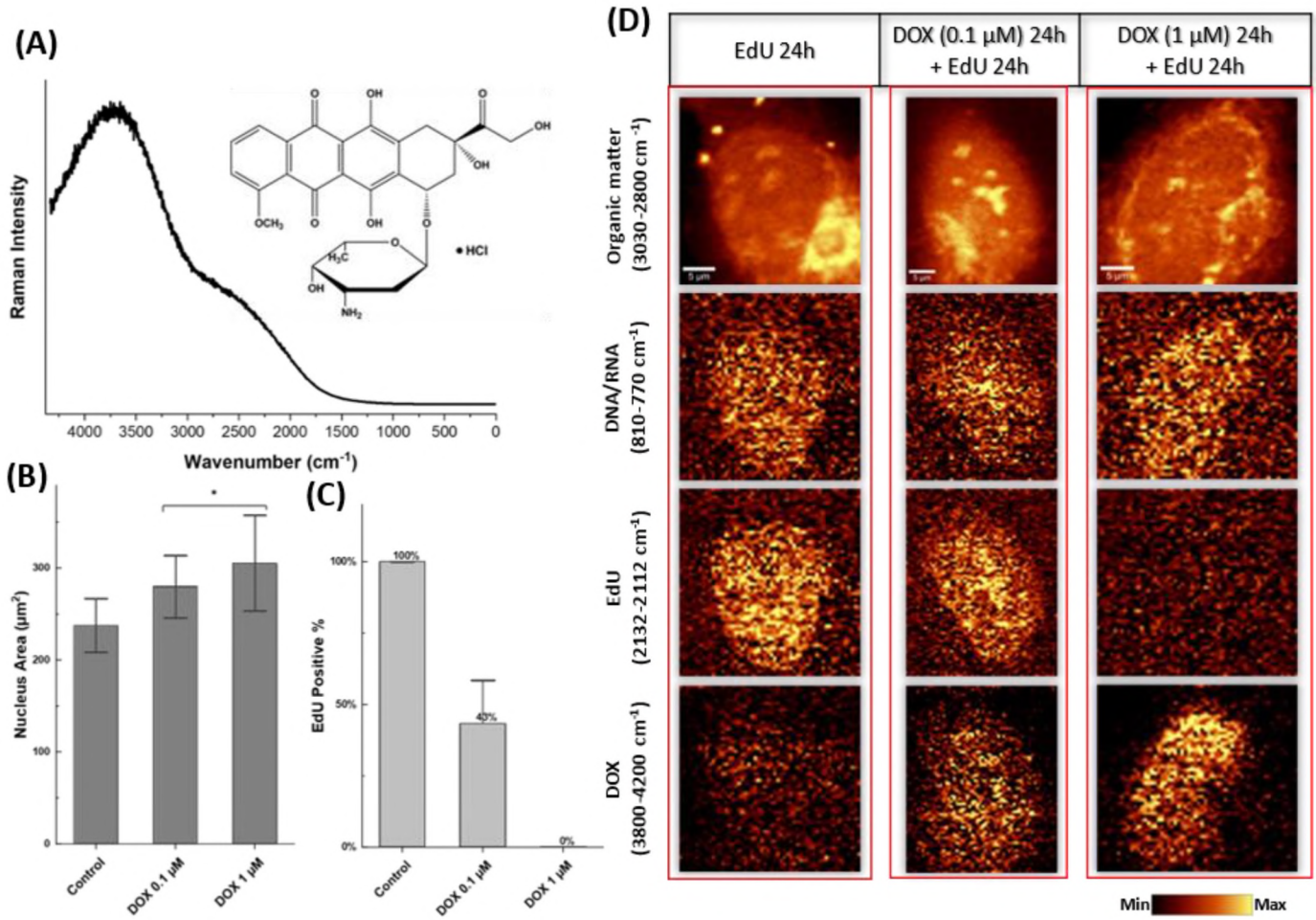

Fig. 6. Raman imaging study of Doxorubicin antiproliferative effect on EC. (A) Structure and Raman spectrum of doxorubicin hydrochloride (DOX), measured using 488 nm excitation wavelength. **(B)** Mean (±SD) nucleus area of control and DOX pre-treated HMEC-1 cells, *P < 0.05 *vs.* control. **(C)** percentage of EdU-positive HMEC-1 cells (that express a Raman band at ca. 2122 cm^{-1}) to the total number of cells (based on the nucleic acids band at ca. 788 cm^{-1}). **(D)** Raman images of EdU-labelled (20 μM, 24h) control and DOX pre-treated (0.1 and 1 μM, 24h) HMEC-1 cells obtained by the integration of Raman bands at: 3030–2800 cm^{-1} (organic matter), 810–770 cm^{-1} (DNA/RNA), 2132–2112 cm^{-1} (Alkyne group, EdU), and 4200–3800 cm^{-1} (DOX), scale bars equal 5 μm.

clear localization of EdU in cell nuclei was observed (Fig. 1B). EdU was detectable in EC nuclei after 3 h of incubation time, however, both the count of EdU positive cells and the intensity of the alkyne band at ca 2122 cm^{-1} increased after 24h incubation with EdU. Furthermore, the integration of the Raman spectra of cells at the spectral region around 2122 cm^{-1}, in the samples treated with EdU for 24h, shows distinct improvement of nuclei imaging compared to following nucleic acids Raman band at ca. 788 cm^{-1}.

Endothelial cells in different organs show a great deal of heterogeneity, moreover, they are subjected to different environments and are influenced by their surroundings, which contributes to their morphological and functional differences (Reiterer and Branco, 2020; Ribatti et al., 2021). To investigate the potential of EdU and improve Raman imaging of cell nuclei of EC from different origins that show, among others, differences in cell proliferation rates, we studied EdU distribution in human microvascular endothelial cells (HMEC-1), human aortic endothelial cells (HAoEC) and human coronary artery endothelial cells (HCAEC). Relatively better images of EC nuclei were obtained by the integration of the Raman band at ca. 2122 cm^{-1} (EdU) in EdU-tagged EC regardless of their origin (Fig. 1B).

3.2. *Live endothelial cell imaging - advantage of the Raman imaging approach to track cell proliferation*

Since the distribution of EdU based on the peak arising from its alkyne tag was clearly detectable in the silent region of the Raman spectra of EC (as shown in Figs. 1A and 2B), a click-free manner of EdU detection was possible allowing live-cell imaging and bypassing the effects of fixation on cells. This was an important issue, as for instance, glutaraldehyde fixation decreased the intensity of the characteristic nucleic acid band at ca. 785 cm^{-1} as well as the DNA marker band at ca. 1096 cm^{-1} assigned for O–P–O stretching mode (Bik et al., 2020). As shown in Fig. 2, EdU-labelled DNA in live HMEC-1 cells was detected based on its characteristic band at ca. 2122 cm^{-1} in live-cell proliferation assay. This highlights one of the advantages of the Raman imaging-based method to detect cell proliferation i.e. the ability to image EdU-tagged live cells due to the lack of necessity for additional dyes to detect EdU. Whereas for fluorescence-based detection, a click chemistry reaction following cell fixation and permeabilization is needed for the subsequent detection of EdU-labelled cellular DNA.

3.3. *Raman imaging-based EdU cell proliferation assay following DNA synthesis inhibition*

CHX inhibits protein synthesis that subsequently results in decreased detection of EdU-positive cells (Henriksson et al., 2018). To assess whether Raman imaging-based EC proliferation assay is sensitive to changes induced by CHX treatment, we incubated HMEC-1 with EdU in the cell culture medium (20 μM), in the absence or presence of CHX added for 60 min at 1 and 10 μg/ml concentrations. Raman imaging of

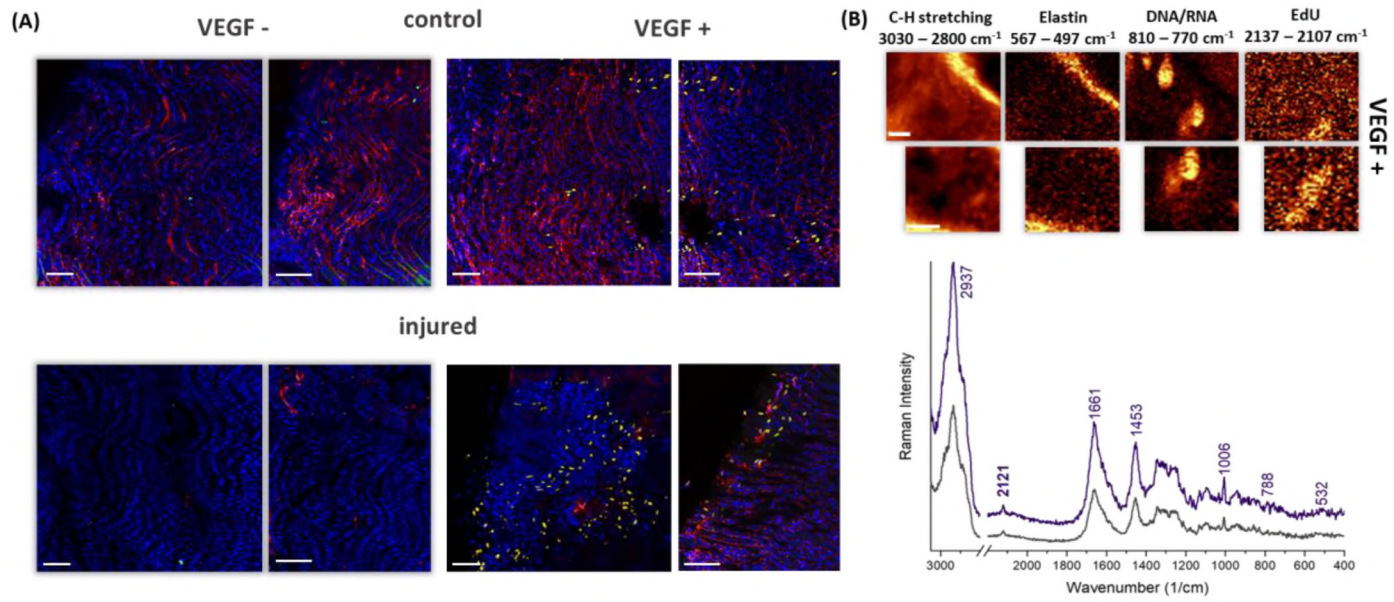

Fig. 7. Raman and fluorescence imaging of EC and SMC regeneration in *en face* murine aorta. (A) Fluorescence images of control and injured murine aorta incubated with MEM for 48h (with and without VEGF supplementation), stained for endothelial marker CD31 (red), nuclei marker Hoechst (blue), and EdU (yellow). **(B)** Raman images of EdU-tagged uninjured *en face* aorta (incubated with VEGF-supplemented MEM for 48h) showing organic matter (3030–2800 cm^{-1}), elastin (567–497 cm^{-1}), DNA/RNA (810–770 cm^{-1}), and EdU (2132–2112 cm^{-1}), and the corresponding average spectra of the EdU-positive nuclei; average spectra of the EdU-positive nucleus on the top panel (top, purple), average spectra of the EdU-positive nucleus on the bottom panel (bottom, grey).

control HMEC-1 incubated with EdU for 24h showed a clear distribution of EdU, to be seen by following the alkyne band at ca. 2122 cm^{-1} (Fig. 3A). Cells that were pre-treated with CHX demonstrated the decreased intensity of the characteristic EdU band at ca. 2122 cm^{-1}, especially in the case of the group pre-treated with a higher concentration of CHX (10 μg/ml) (Fig. 3B), where a considerable number of cells did not exhibit any EdU signal.

Through cluster analysis of the Raman images of EC, the average spectra of cell nuclei in each group were collected and compared. As shown in Fig. 3B, there was a considerable decrease in the intensity of the band associated with EdU in the CHX (10 μg/ml) pre-treated cells compared to control, whereas the decrease was minor in the group pre-treated with lower (1 μg/ml) concentration of CHX. However, the characteristic nucleic acids band at ca. 788 cm^{-1} did not show a significant change in the CHX pre-treated groups compared to the control. This demonstrates the inhibition of EC proliferation in the CHX pre-treated group (10 μg/ml), without a significant change to the already formed DNA in EC nuclei.

To quantify the percentage of the EdU-positive cell population in each group, a larger area of cells was scanned using shorter image acquisition times. Afterwards, cells were counted in each measurement and judged by the presence or absence of the characteristic EdU band at ca. 2122 cm^{-1} in their respective nuclei. The nucleic acid characteristic band at ca. 788 cm^{-1} was used as a reference to count the total number of cells in all the samples. By analysing the Raman spectra of the measured cells, a significant decrease in EdU-positive cell count was observed in the group of cells pre-treated with CHX (10 μg/ml), compatible with the inhibition of DNA synthesis (Fig. 4B). These experiments demonstrated that Raman imaging-based EdU assay for endothelial cells proliferation was sensitive to CHX inhibition as expected (Henriksson et al., 2018).

3.4. *Fluorescence imaging as a reference method for inhibition of cell proliferation*

For comparison, we utilized fluorescent detection of Alexa Fluor® 488-stained EdU in HMEC-1 incubated with EdU in similar experimental conditions in the absence and presence of CHX (1 and 10 μg/ml, 1h). We observed that the percentage of EdU-positive HMEC-1 decreased significantly in the group of cells pre-treated with CHX higher concentration (10 μg/ml) as compared to control cells (Fig. 5B). Furthermore, the intensity of the signal from Alexa Fluor has shown a significant decrease in that same group compared to control cells, as shown in Fig. 5C. Both the percentage of EdU-positive cells and the intensity of the Alexa Fluor signal from EC nuclei treated with a lower concentration of CHX (1 μg/ml) decreased to a lesser degree. These results correlate with the Raman imaging results supporting the equivalence of the Raman imaging-based click-free approach to assay endothelial cell proliferation as compared to the classical fluorescence-based approach. Some of the differences observed between the fluorescence and Raman-based techniques in EdU detection can be attributed to a number of reasons, including the differences in sample preparation using different substrates for cell culture, a difference in the detection method (click free *vs.* click chemistry based), and to some degree, difference in thresholding.

3.5. *EdU labelled Raman-based detection of doxorubicin effect on EC*

Doxorubicin induces pronounced cellular toxicity at nuclear, cytosolic and membrane levels in endothelial cells *in vitro* (Dębowska et al., 2016; Majzner et al., 2015; Wojcik et al., 2015). In particular, the accumulation of doxorubicin in endothelial nuclei and increased nuclear area were prominent features of doxorubicin endothelial toxicity. In line with these previous reports, as shown in Fig. 6B, the mean nucleus area increased significantly in DOX-treated endothelial cells as compared to control cells and this effect was associated with DOX accumulation in EC nuclei. The increase in nucleus area, as well as the elevation of background in the high wavenumber range in the Raman spectra (ca. 4200–3800 cm^{-1}), was more pronounced with higher DOX concentration. Interestingly, using Raman imaging-based EdU assay we detected antiproliferative effect of DOX on HMECs with the lower concentration of DOX (0.1 μM) resulting in partial inhibition of proliferation, while the higher DOX concentration (1 μM) caused a complete blocking of cell proliferation (Fig. 6C).

Of note, in control endothelial cells and in endothelial cells treated with the lower concentration of DOX, EdU-based images of cell nuclei resulting from EdU signal at ca. 2122 cm^{-1} were very well visible while

higher DOX concentration endowed with pronounced cytotoxicity impaired the signal detection. These results suggest that EdU-based Raman imaging may prove useful to study morphological changes in EC nuclei in addition to detecting changes in cell proliferation.

3.6. Detection of ex vivo proliferation of endothelial cells and smooth muscle cells in isolated murine aorta

To assess the applicability of Raman imaging-based EdU assay for endothelial cells proliferation or regeneration of endothelial cells *in situ* aortic rings from isolated murine aorta were subjected to mechanical injury and then incubated *ex vivo* in media with and without VEGF supplementation. After 48h of incubation with EdU, the group of samples without VEGF supplementation showed negligible EdU incorporation, while EdU-positive cells were detected in the group of samples incubated with VEGF in their culture medium. EdU-positive cells were detected in the control (non-injured) aorta samples, however, the number of EdU-positive cells was greater in the injured aortae. To determine whether the EdU signal was detected in the endothelium, PECAM-1 (platelet/endothelial cell adhesion molecule-1, CD-31) immunostaining, which is widely used for endothelial differentiation, was performed. The majority of proliferating cells were found to be CD-31 negative with elongated nuclei, which could be attributed to smooth muscle cells (SMCs). However, a smaller number of EdU-positive, CD-31 positive cells were detected as well (Fig. 7A).

Raman imaging of *en face* aorta samples showed a few detectable EdU-positive cells without the need for additional staining (Fig. 7B). Although imaging of cell nuclei in *en face* aorta samples is possible using label-free Raman detection of the band at ca. 788 cm^{-1}, the differentiation between proliferating and non-proliferating cells was only possible by detecting the alkyne band in EdU-positive cells at ca. 2122 cm^{-1}.

4. Conclusions

Here we describe a novel method to study EC proliferation by Raman-based imaging of EdU as a click-free Raman probe for DNA synthesis. Comprehensive information on the incorporation of EdU in EC DNA was obtained, allowing the quantification of EdU-positive cells while keeping the spectral information (obtainable with label-free Raman imaging) intact. The results of the EdU labelled Raman imaging to detect EC proliferation were confirmed using fluorescence microscopy. Importantly, the Raman imaging-based approach omits the cell permeabilization step and allows the tracking of EdU in EC without the need for the fluorescent azide dye (in a click-free manner), permitting live-cell imaging. On the other hand, the limitations of this technique include the longer image acquisition times (ca. 30–40 min/image) compared to fluorescence imaging. However, relying on nonlinear Raman techniques such as stimulated Raman scattering (SRS) and coherent anti-Stokes Raman scattering (CARS) would potentially improve the imaging speed of EdU-tagged cell nuclei (Wei et al., 2014; Yamakoshi et al., 2011).

The known limitations of the fluorescence imaging-based method include the limited number of dyes that could be used simultaneously, the risk of photobleaching and the reliance on the click chemistry reaction. In this context, the Raman and fluorescence-based techniques each have their advantages and limitations and could be regarded as complementary methods, with fluorescence imaging offering a bigger picture overview of the state of the samples and Raman imaging offering a more detailed assessment with minimal effects on the relatively fragile EC samples.

Of note, Raman imaging-based detection of EdU-labelled nuclei could be also applied to the *ex vivo* murine aortae model as shown here. Nonetheless, the sensitivity of this technique needs improvement and optimization e.g. to utilize new Rp for DNA synthesis that may offer better signal enhancement such as resonance Rp or by developing different alkynes and azides utilizing click chemistry for subsequent Raman detection of EC proliferation.

Authors contribution

MB, SC, EM and **BR** conceived and designed the experiments; **BR, MSternak** and **SR** performed sample preparations; **BR** and **KB** performed Raman imaging; **SR** and **BR** performed staining and fluorescence imaging; **MStodulski** and **RP** synthesized samples for Click Chemistry and **JM** supervised the work; **BR** analysed the data; **BR** and **MB** wrote the manuscript; **BR** visualized the data; **MB** supervised the work. All authors reviewed the manuscript.

Declaration of competing interest

The authors declare that they have no known competing financial interests or personal relationships that could have appeared to influence the work reported in this paper.

Data availability

Data will be made available on request.

Acknowledgements

The study was supported by the European Union's Horizon 2020 Research and Innovation Programme under Marie Sklodowska-Curie [Grant Agreement 813920 (LogicLab ITN)] and by the National Science Center Poland (NCN) [OPUS15 no. UMO-2018/29/B/ST4/00335 to MB].

The authors are grateful to MSc Renata Budzynska (JCET UJ) for cell culture maintenance, and to MSc Adrianna Wislocka-Orlowska and Wieslawa Krynicka for technical support.

References

Adamczyk, A., Matuszyk, E., Radwan, B., Rocchetti, S., Chlopicki, S., Baranska, M., 2021. Toward Raman subcellular imaging of endothelial dysfunction. J. Med. Chem. 64, 4396–4409. https://doi.org/10.1021/acs.jmedchem.1c00051.

Baranska, M., Kaczor, A., Malek, K., Jaworska, A., Majzner, K., Staniszewska-Slezak, E., Pacia, M.Z., Zajac, G., Dybas, J., Wiercigroch, E., 2015. Raman microscopy as a novel tool to detect endothelial dysfunction. Pharmacol. Rep. 67, 736–743. https://doi.org/10.1016/j.pharep.2015.03.015.

Basile, D.P., Friedrich, J.L., Spahic, J., Knipe, N., Mang, H., Leonard, E.C., Changizi-Ashtiyani, S., Bacallao, R.L., Molitoris, B.A., Sutton, T.A., 2011. Impaired endothelial proliferation and mesenchymal transition contribute to vascular rarefaction following acute kidney injury. Am. J. Physiol. Physiol. 300, F721–F733. https://doi.org/10.1152/ajprenal.00546.2010.

Bik, E., Dorosz, A., Mateuszuk, L., Baranska, M., Majzner, K., 2020. Fixed versus live endothelial cells: the effect of glutaraldehyde fixation manifested by characteristic bands on the Raman spectra of cells. Spectrochim. Acta Part A Mol. Biomol. Spectrosc. 240, 118460 https://doi.org/10.1016/j.saa.2020.118460.

Cau, S.B.A., Evora, P.R.B., Tostes, R.C., 2018. Vasoconstrictor substances produced by the endothelium. In: Da Luz, P.L., Libby, P., Chagas, A.C.P., Laurindo, F.R.M. (Eds.), Endothelium and Cardiovascular Diseases. Elsevier, pp. 115–125. https://doi.org/10.1016/B978-0-12-812348-5.00009-X.

Czamara, K., Adamczyk, A., Stojak, M., Radwan, B., Baranska, M., 2021. Astaxanthin as a new Raman probe for biosensing of specific subcellular lipidic structures: can we detect lipids in cells under resonance conditions? Cell. Mol. Life Sci. 78, 3477–3484. https://doi.org/10.1007/s00018-020-03718-1.

Czamara, K., Petko, F., Baranska, M., Kaczor, A., 2016. Raman microscopy at the subcellular level: a study on early apoptosis in endothelial cells induced by Fas ligand and cycloheximide. Analyst 141, 1390–1397. https://doi.org/10.1039/C5AN02202A.

Daiber, A., Chlopicki, S., 2020. Revisiting pharmacology of oxidative stress and endothelial dysfunction in cardiovascular disease: evidence for redox-based therapies. Free Radic. Biol. Med. 157, 15–37. https://doi.org/10.1016/j.freeradbiomed.2020.02.026.

Deanfield, J.E., Halcox, J.P., Rabelink, T.J., 2007. Endothelial function and dysfunction. Circulation 115, 1285–1295. https://doi.org/10.1161/CIRCULATIONAHA.106.652859.

Dębowska, K., Dębski, D., Michałowski, B., Dybala-Defratyka, A., Wójcik, T., Michalski, R., Jakubowska, M., Selmi, A., Smulik, R., Piotrowski, Ł., Adamus, J., Marcinek, A., Chlopicki, S., Sikora, A., 2016. Characterization of fluorescein-based monoboronate probe and its application to the detection of peroxynitrite in

endothelial cells treated with doxorubicin. Chem. Res. Toxicol. 29, 735–746. https://doi.org/10.1021/acs.chemrestox.5b00431.
Galley, H.F., Webster, N.R., 2004. Physiology of the endothelium. Br. J. Anaesth. 93, 105–113. https://doi.org/10.1093/bja/aeh163.
Henriksson, S., Groth, P., Gustafsson, N., Helleday, T., 2018. Distinct mechanistic responses to replication fork stalling induced by either nucleotide or protein deprivation. Cell Cycle 17, 568–579. https://doi.org/10.1080/15384101.2017.1387696.
Huertas, A., Montani, D., Savale, L., Pichon, J., Tu, L., Parent, F., Guignabert, C., Humbert, M., 2020. Endothelial cell dysfunction: a major player in SARS-CoV-2 infection (COVID-19)? Eur. Respir. J. 56, 2001634 https://doi.org/10.1183/13993003.01634-2020.
Ishizuka, T., Liu, H.S., Ito, K., Xu, Y., 2016. Fluorescence imaging of chromosomal DNA using click chemistry. Sci. Rep. 6, 33217 https://doi.org/10.1038/srep33217.
Kim, H.-S., Lee, Y.-S., Kim, D.-K., 2009. Doxorubicin exerts cytotoxic effects through cell cycle arrest and fas-mediated cell death. Pharmacology 84, 300–309. https://doi.org/10.1159/000245937.
Liu, S.J., Melchert, R.B., 2010. In vitro cultured cardiomyocytes for evaluating cardiotoxicity. In: Comprehensive Toxicology. Elsevier, pp. 113–131. https://doi.org/10.1016/B978-0-08-046884-6.00706-5.
Liu, X., Yang, J.-M., Zhang, S.S., Liu, X.-Y., Liu, D.X., 2010. Induction of cell cycle arrest at G1 and S phases and cAMP-dependent differentiation in C6 glioma by low concentration of cycloheximide. BMC Cancer 10, 684. https://doi.org/10.1186/1471-2407-10-684.
Majzner, K., Wojcik, T., Szafraniec, E., Lukawska, M., Oszczapowicz, I., Chlopicki, S., Baranska, M., 2015. Nuclear accumulation of anthracyclines in the endothelium studied by bimodal imaging: fluorescence and Raman microscopy. Analyst 140, 2302–2310. https://doi.org/10.1039/C4AN01882F.
Maslak, E., Gregorius, A., Chlopicki, S., 2015. Liver sinusoidal endothelial cells (LSECs) function and NAFLD; NO-based therapy targeted to the liver. Pharmacol. Rep. 67, 689–694. https://doi.org/10.1016/j.pharep.2015.04.010.
Matuszyk, E., Adamczyk, A., Radwan, B., Pieczara, A., Szcześniak, P., Mlynarski, J., Kamińska, K., Baranska, M., 2021. Multiplex Raman imaging of organelles in endothelial cells. Spectrochim. Acta Part A Mol. Biomol. Spectrosc. 255, 119658 https://doi.org/10.1016/j.saa.2021.119658.
Radwan, B., Adamczyk, A., Tott, S., Czamara, K., Kaminska, K., Matuszyk, E., Baranska, M., 2020. Labeled vs. Label-free Raman imaging of lipids in endothelial cells of various origins. Molecules 25, 5752. https://doi.org/10.3390/molecules25235752.
Rajendran, P., Rengarajan, T., Thangavel, J., Nishigaki, Y., Sakthisekaran, D., Sethi, G., Nishigaki, I., 2013. The vascular endothelium and human diseases. Int. J. Biol. Sci. 9, 1057–1069. https://doi.org/10.7150/ijbs.7502.
Reiterer, M., Branco, C.M., 2020. Endothelial cells and organ function: applications and implications of understanding unique and reciprocal remodelling. FEBS J. 287, 1088–1100. https://doi.org/10.1111/febs.15143.
Ribatti, D., Tamma, R., Annese, T., 2021. The role of vascular niche and endothelial cells in organogenesis and regeneration. Exp. Cell Res. 398, 112398 https://doi.org/10.1016/j.yexcr.2020.112398.
Ruhl, L., Pink, I., Kühne, J.F., Beushausen, K., Keil, J., Christoph, S., Sauer, A., Boblitz, L., Schmidt, J., David, S., Jäck, H.-M., Roth, E., Cornberg, M., Schulz, T.F., Welte, T., Höper, M.M., Falk, C.S., 2021. Endothelial dysfunction contributes to severe COVID-19 in combination with dysregulated lymphocyte responses and cytokine networks. Signal Transduct. Targeted Ther. 6, 418. https://doi.org/10.1038/s41392-021-00819-6.
Salic, A., Mitchison, T.J., 2008. A chemical method for fast and sensitive detection of DNA synthesis in vivo. Proc. Natl. Acad. Sci. U.S.A. 105, 2415–2420. https://doi.org/10.1073/pnas.0712168105.
Siegel, M.R., Sisler, H.D., 1963. Inhibition of protein synthesis in vitro by cycloheximide. Nature 200, 675–676. https://doi.org/10.1038/200675a0.
Smeda, M., Chlopicki, S., 2020. Endothelial barrier integrity in COVID-19-dependent hyperinflammation: does the protective facet of platelet function matter? Cardiovasc. Res. 116, e118–e121. https://doi.org/10.1093/cvr/cvaa190.
Smeda, M., Przyborowski, K., Stojak, M., Chlopicki, S., 2020. The endothelial barrier and cancer metastasis: does the protective facet of platelet function matter? Biochem. Pharmacol. 176, 113886 https://doi.org/10.1016/j.bcp.2020.113886.
Taymaz-Nikerel, H., Karabekmez, M.E., Eraslan, S., Kırdar, B., 2018. Doxorubicin induces an extensive transcriptional and metabolic rewiring in yeast cells. Sci. Rep. 8, 13672 https://doi.org/10.1038/s41598-018-31939-9.
Walczak, M., Suraj, J., Kus, K., Kij, A., Zakrzewska, A., Chlopicki, S., 2015. Towards a comprehensive endothelial biomarkers profiling and endothelium-guided pharmacotherapy. Pharmacol. Rep. 67, 771–777. https://doi.org/10.1016/j.pharep.2015.06.008.
Wei, L., Hu, F., Shen, Y., Chen, Z., Yu, Y., Lin, C.-C., Wang, M.C., Min, W., 2014. Live-cell imaging of alkyne-tagged small biomolecules by stimulated Raman scattering. Nat. Methods 11, 410–412. https://doi.org/10.1038/nmeth.2878.
Wojcik, T., Buczek, E., Majzner, K., Kolodziejczyk, A., Miszczyk, J., Kaczara, P., Kwiatek, W., Baranska, M., Szymonski, M., Chlopicki, S., 2015. Comparative endothelial profiling of doxorubicin and daunorubicin in cultured endothelial cells. Toxicol. Vitro 29, 512–521. https://doi.org/10.1016/j.tiv.2014.12.009.
Yamakoshi, H., Dodo, K., Okada, M., Ando, J., Palonpon, A., Fujita, K., Kawata, S., Sodeoka, M., 2011. Imaging of EdU, an alkyne-tagged cell proliferation probe, by Raman microscopy. J. Am. Chem. Soc. 133, 6102–6105. https://doi.org/10.1021/ja108404p.